PHILOSOPHICAL MAGAZINE
2024, VOL. 104, NOS. 9–10, 482–498
https://doi.org/10.1080/14786435.2024.2310570

Unifying the size effect observed in micropillar compression experiments

Halil Yilmaz[a,b] and Brian Derby[a]

[a]Department of Materials, University of Manchester, Manchester, UK; [b]Department of Mechanical and Metal Technologies, Mus Alparslan University, Mus, Turkey

ABSTRACT

Micropillar compression experiments show size effect, $\sigma_p/\mu = A(d/b)^n$, where σ_p, is the flow stress, μ is the resolved shear modulus, d is the pillar diameter and b is Burgers' vector. With fcc metals $n \approx -0.67$ and $A \approx 0.7$; however, with bcc metals there is greater variation, with n closer to zero. Here we propose a different but similar empirical relation of $\sigma_p/\mu = \sigma_b/\mu + A'(d/b)^{n'}$, where σ_b is a size independent resistance stress. In which case there must be a strong correlation between the original constants, A and n. This hypothesis is found to be true for the published data from a large number of bcc metals, ionic solids that possess the rock salt crystal structure, and some covalent bonded semiconductors. This correlation is shown to predict a universal power law with the exponent in the range, $-1.0 < n' < -0.5$, and with A' close to 1. These values are very similar to the empirical relation that can be used to describe the behaviour of fcc metals tested in micropillar compression with $\sigma_b = 0$. This universality of the empirical relation provides strong evidence for a common mechanism for the micropillar size effect across a range of materials.

ARTICLE HISTORY
Received 4 July 2023
Accepted 18 January 2024

KEYWORDS
Plastic deformation; micropillar compression test; body centred cubic metals; ionic solids; strong solids

1. Introduction

Size effects are well known phenomena in materials science. These can result from the finite size of a structure; e.g, in the case of brittle fracture, where Griffiths' equation shows that strength is controlled by the dimensions of largest defect present. In which case, the maximum defect size and hence minimum strength, is determined by the physical dimensions of a component. In polycrystalline metals, plastic flow is inversely related to the size of the crystalline grains through the Hall-Petch relation that states that the strength is here

CONTACT Brian Derby brian.derby@manchester.ac.uk Department of Materials, University of Manchester, Oxford Rd, Manchester M13 9PL, UK

Supplemental data for this article can be accessed online at https://doi.org/10.1080/14786435.2024.2310570.

related to the inverse of the grain size to the power of 0.5. In both examples, the trend is clear that smaller means stronger. Size dependent behaviour of deformation has also been observed with the epitaxial growth of crystalline thin films where strain relief through misfit dislocations occurs at a critical thickness. This behaviour has been explained through the reduction in strain energy being balanced by the elastic fields of the strain relieving dislocations [1] and also by geometrical arguments relating to crystalline slip and the magnitude of the Burgers vector [2]. Similar results showing this size dependent strengthening behaviour have been reported for the torsion of metal wires [3], the bending of thin films [4] and the hardness of nanoindentations [5]. In these three examples, the strengthening behaviour has been explained by the presence of gradients in plastic strain, which must be accommodated by a population of 'geometrically necessary dislocations' that form to accommodate gradients of plastic strain [6].

More recently, a distinct size effect of the plastic flow stress measured during micropillar compression experiments when the diameter of the pillar sample is smaller than about 5 μm was first reported by Uchic et al. with experiments on Ni [7]. This configuration does not introduce a significant gradient in plastic strain, unlike earlier reports on twisting and bending of small metal structures [3–5]. This phenomenon was confirmed following further experiments on a range of face centred cubic (fcc) structure metals, all confirming a considerable increase in the plastic flow stress as the pillar diameter decreases [8–11].

The experimental data from micropillar compression experiments has been commonly reported using the following empirical power law relating the plastic flow stress, σ_p, to the pillar diameter, d, with

$$\sigma_p = \alpha d^n \tag{1}$$

Where, α and n are experimentally determined constants. Dou and Derby reviewed the published data for fcc metals and noted that the power law exponent, n, ranged over a relatively small range, between −0.8 and −0.6 [12]. They further proposed that, if the plastic flow stress was normalised by the shear modulus resolved along the direction and plane of the active slip system, μ, and the pillar diameter was normalised by the Burgers vector, b, then all the published data for fcc metal micropillar compression experiments lay in a narrow region of the parameter space, with all the data described by a 'universal relation', with.

$$\frac{\sigma_p}{\mu} = A\left(\frac{d}{b}\right)^n \tag{2}$$

Where, $n = -0.67$, and $A = 0.71$, a dimensionless constant. This behaviour has been confirmed by other, more comprehensive, reviews of the literature, [13] which concluded that the size effect was real and cannot be readily explained by mechanisms such as strain gradients or dislocation confinement.

Despite this empirical relationship, there is no agreement in the literature as to the mechanism that leads to this size dependent behaviour. Conventional, obstacle based, dislocation bowing mechanisms of strengthening predict and inverse relation with the appropriate length scale. A similar inverse relationship is also predicted by earlier work on stress relief in thin films. If the strengthening mechanism requires the cutting of a physical barrier (e.g. grain boundary penetration or crack propagation), stresses are expected to scale with dimension following an exponent of −0.5, as is also the case when the barrier is a forest of dislocations, whether generated by plastic deformation or geometrical necessity [14]. Two, quite different mechanisms have been proposed for the case of micropillar compression, neither of which produces a predictive model that mimics the observed size dependence of strength. The first mechanism, proposed by Greer and Nix, suggested that the close proximity of the free surfaces in a small cylindrical single crystal, specimen allows easy dislocation escape during deformation [15]. This, so called, dislocation starvation or mechanical annealing mechanism, requires the continuous nucleation of new dislocations for the deformation to continue. Some transmission electron microscopy (TEM) experiments tracking dislocation migration during the *in situ* deformation of metal micropillars have demonstrated that this may occur [16,17]. Parthasarathy et al. proposed another mechanism that modelled the effect of the confinement of the pillar diameter on the classical Frank-Read, pinned dislocation line, model for dislocation multiplication [18]. Here it was proposed that, at small pillar diameters, the length of a typical dislocation source will be larger than the diameter of the pillar. In which case a modified source geometry of a single pinned end with the other, mobile dislocation, end intersecting the free surface. The motion of this 'single end source' generates new dislocations, with an effective length determined by its distance to the surface and the effective mean length now a function of the pillar diameter. There has also been published TEM data to support this mechanism [17]. However, although Parthasarathy's model predicts a high strength, the single source arm is still limited by the dimensions of the pillar and hence a size exponent of −1 is still implied.

There have been fewer reports in the literature on the behaviour of metals with crystal structures other than fcc. However, it is clear from the data in the literature, that the micropillar compression deformation of body centred cubic (bcc) structured metals, show much less uniformity between different metals than was found with the fcc metals. It is generally found that bcc metals have significantly greater yield and plastic flow stress values than are found with fcc metals. In addition, the specimen size effect is less apparent than the fcc phenomenon, with a much smaller influence of specimen diameter and the equivalent size effect exponent in the range $-0.6 < n < -0.2$ [19–21].

Schneider et al. noted that there appeared to be a systematic correlation between the micropillar compression size effect exponent reported for BCC metals and the critical temperature for screw dislocation mobility, T_c. Below this temperature, BCC materials are considerably stronger because the dislocation core structure of a screw dislocation requires thermal activation for dislocation migration [21]. For BCC metals tested at room temperature, the exponent n tended to a value close to the fcc mean value, if T_c was close to room temperature, while if T_c was significantly greater than room temperature then the value of n was larger and the size effect reduced.

Korte and Clegg extended micropillar compression studies beyond metals to semiconductors (Si and GaAs) and ionic crystals (MgO and LiF). In all these cases they found that the measured micropillar compression size effect was considerably smaller than observed with fcc metals [22]. Korte and Clegg correlated the reduction in size effect to the equivalent plastic flow stress in the bulk material, i.e. specimens with dimensions considerably greater than the diameter of the pillars used in micropillar compression experiments, which is considerably greater than is the case for metal specimens. This is effectively the same correlation as noted by Schneider, because the proximity to the critical temperature is a proxy for the bulk stress of a bcc metal. For such stronger classes of materials compared to the fcc structure metals, Korte and Clegg suggested that equation 2 presents an oversimplified description of the size effect, which is better represented by an equation of the form:

$$\sigma_p - \sigma_b = \alpha' d^{n'} \tag{3a}$$

or in dimensionless form

$$\frac{\sigma_p - \sigma_b}{\mu} = A' \left(\frac{d}{b}\right)^{n'} \tag{3b}$$

Where, σ_b represents a 'bulk stress' or the stress displayed by the material in the absence of any size dependent behaviour. Thus, with this formulation, the size effect is considered additive to the underlying or intrinsic stress of a material.

2. Size effects, intrinsic strength and power laws

Many studies of the size effect found during micropillar compression experiments on BCC metals and other high strength materials have considered whether a relation in the form of equation 3 provides an appropriate description of the observed behaviour. Parthasarathy et al. [18] presented a model where the strength of a metal is controlled by the length scale associated with a (Frank-Read) dislocation source in addition to a strength contribution from Taylor hardening. At small pillar diameters the dislocation sources are truncated by the free surfaces and the length scale transitions to a function of the pillar diameter. This leads to a strength size relation of the form:

With

$$\sigma_p = f(d) + f(\rho) \tag{4}$$

where, ρ, is the dislocation density. The *f(d)* term is derived from a statistical argument for the mean distance between a dislocation source and the free surface, which has a complex integral form but is only important with the pillar size is smaller than about 10^{-5} m. The second term, $f(\rho)$ is not a materials constant but is considered independent of the physical size of the specimen. The model showed excellent results when compared with experimental data from experiments on Au and Ag specimens.

This expression can be readily extended to high bulk strength materials, such as BCC structure metals, ceramics and semiconductors by the inclusion of a second size independent term identified as the lattice resistance to dislocation motion. This is associated with thermally activated screw dislocation mobility in BCC materials and other impediments to dislocation motion associated with the lattice resistance to dislocation glide in strong materials. The plastic flow stress is broken down into three components, following the initial approach of Parthasarathy et al. [18] These are:

1) A size dependent component, *f(d)*, which may be based on a mechanism (e.g. Parthasarathy's single arm source) or be empirical.
2) The bulk resistance to plastic flow, which here is represented by a Taylor hardening or dislocation density term, $f(\rho)$.
3) A constant lattice resistance to plastic flow (sometimes called the bulk stress), σ_b, which is a function of testing temperature.

With

$$\sigma_p = f(d) + f(\rho) + \sigma_b \tag{5}$$

This has been used successfully in a number of prior studies to interpret the size effect observed during micropillar compression experiments with BCC metals, [24,25] ionic crystals (LiF), [26] and Si [27]. In all cases there is a reasonable agreement between the formulation and experimental data.

If the true relationship between the compression strength of a micropillar is described by equations in the form of equations 3–5, then the method used to display the experimental data obtained from a series of micropillar compression tests as a log/log plot of strength as a function of pillar diameter will not produce a linear relation. This was noted by Lee and Nix, who observed that if such a plot was made and a linear relation was assumed from the experimental data plotted on logarithmic axes, the apparent gradient, *n*, will be different from that of equation 3 with $n > n'$ [23]. This is clear from manipulating equation 3, resulting in.

$$\frac{d\left(\log\frac{\sigma_p}{\mu}\right)}{d\left(\log\frac{d}{b}\right)} = n = n'\frac{(\sigma_p - \sigma_b)}{\sigma_p} \tag{6}$$

Equation 6 predicts that the apparent gradient of the data tends towards zero (increases) as the value of σ_b, the size independent resistance to dislocation motion, increases. This is consistent with Schneider et al.'s observation that the stress exponent in BCC metals decreases as the critical temperature of the metal approaches room temperature [21]. This convergence of the stress exponent in BCC metals, to a value similar to that measured for fcc metals, when the test temperature approaches or exceeds the test temperature has also been reported by Abad et al. [24] with experiments on Ta and W and in our earlier work on Fe, Nb and V [25]. Combining equation 2 and equation 3, then using equation 6 to eliminate σ_b, leads to the following expression

$$logA = \log\frac{\overline{\sigma_p}}{\mu} - \frac{n}{n'}\left[\log\frac{\overline{\sigma_p}}{\mu} + log\frac{n}{n'} - logA'\right] \tag{7}$$

where $\overline{\sigma_p}$ is the mean value of σ_p over which the power law exponent has been measured.

Thus we can see that, if the equation 3 is the correct form of the empirical relationship that relates the strength of BCC micropillars to their diameter and, if the experimental data is plotted with $\log(\sigma_p/\mu)$ as a function of $\log(d/b)$, then the apparent gradient n is strongly correlated with the intercept A and should follow the relation of equation 7 with n' representing an underlying or 'natural' power law exponent and A' the corresponding pre-exponent factor. Here we test this hypothesis using the experimental data published in the literature on the micropillar compression of bcc metals and a range of other materials.

We note here that observations similar to our analysis have also been made by Dunstan and Bushby [28]. They commented on the nature of an apparent power law from the 'uncritical use of logarithmic scales to analyse size effects' during the mechanical deformation of materials. They proposed that all size effects represent a modification of an implicit scale limitation to mechanical strength, critical thickness theory, where the elastic strain limit scales with the dimension of an object normalised by the atomic separation within a crystal. This is stating equation 2 (yield strength/shear modulus = elastic strain) with $n = -1$ as a limiting bound for all size effects. We will return to this in the discussion of our observations.

2.1 Body centred cubic structured metals

There have been a considerable number of reports on the micropillar compression of bcc metals, with pillar diameter < 5 μm. Here we have limited our data survey to pure metals and have not considered any alloy specimens. We have also ensured that there is sufficient information in the experimental work reported to confirm that the data is from single crystal specimens, with a measured orientation and that the testing temperature is reported. All flow stress data has been resolved onto the slip plane with the greatest Schmid factor and normalised by the shear modulus resolved on the slip plane. The pillar diameter is normalised by the Burgers vector of the slip system identified by microscopic observation of pillar deformation. In most cases the authors of the study have measured and reported the power law exponent of the size dependent strength but have not reported the pre-exponent, A. This was determined, where necessary, from the published data by digitising the appropriate data plots. The full data used is presented in the Supplementary Information Table S1 from a range of published reports on micropillar compression experiments carried out on seven different bcc metals (Cr, Fe, Mo, Nb, Ta, V and W) from several literature sources. The testing temperature, T, is also presented in the format $T^* = T/T_c$, where T_c is the critical temperature for screw dislocation mobility used by Schneider et al. [21].

Figure 1a plots the reported size dependent exponent for the strength of bcc metals tested in micropillar compression experiments as a function of the testing temperature, normalised by the critical temperature at which full screw dislocation mobility is attained, $T^* = T/T_c$. This confirms the empirical correlation, first suggested by Schneider et al. [21] but with a much larger range of data from different sources in the literature. However, although the class of bcc metals follows the general trend, for a given metal there is considerable variation in the value of the exponent when data from different studies are compared. This can be reconciled if equation 3 is the appropriate expression to describe the mechanical behaviour of bcc micropillars. Here, the size dependent effect is an additional increment to an intrinsic, size independent or 'bulk material' flow stress. In bcc materials this intrinsic stress is governed by dislocation mobility and, given the thermal activation required for screw dislocation motion, will show a decrease with increasing temperature up to T_c. However, this intrinsic strength is also well known to be highly sensitive to impurities and this can explain the very large variation in the reported stress exponent between different studies of the same metal in the literature at similar values of T^* seen in Figure 1a.

Figure 1b shows strong evidence for the proposed correlation between the size effect exponent, n, and the pre-exponential constant, A, both between different metals and within individual studies of the same metal. This is because equation 7 has eliminated the size independent stress, σ_b. Further

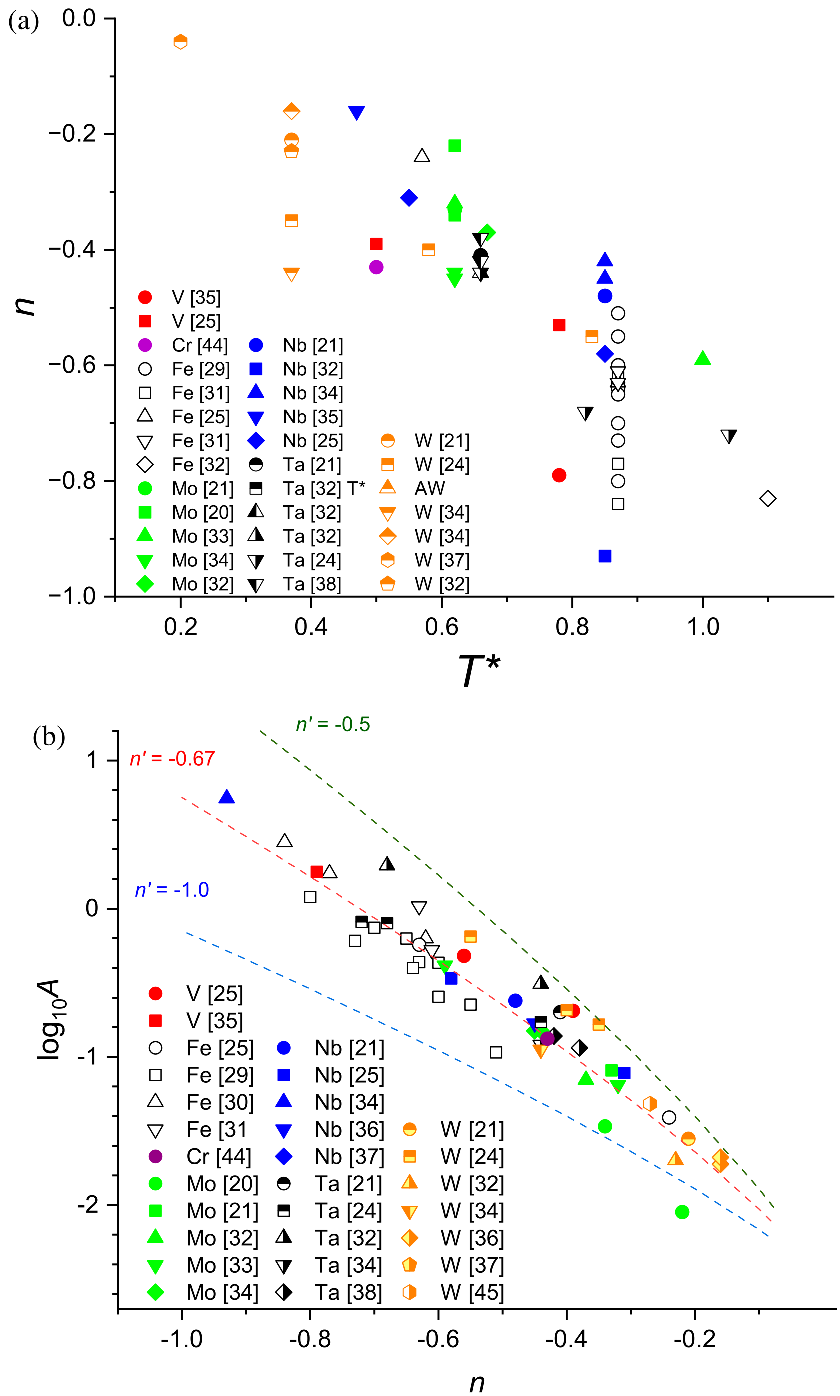

Figure 1. Correlations obtained from mechanical property data from micropillar compression experiments carried out on a range of bcc metals. a) The relationship between the power law exponent, *n*, and testing temperature as a fraction of the critical temperature for the onset of screw dislocation mobility, $T^* = T/T_c$. b) The correlation between the power law exponent and the pre-exponential constant, *A*; the dotted lines are plots of equation 7 for different values of the intrinsic size exponent, *n′*, as defined in equation 3.

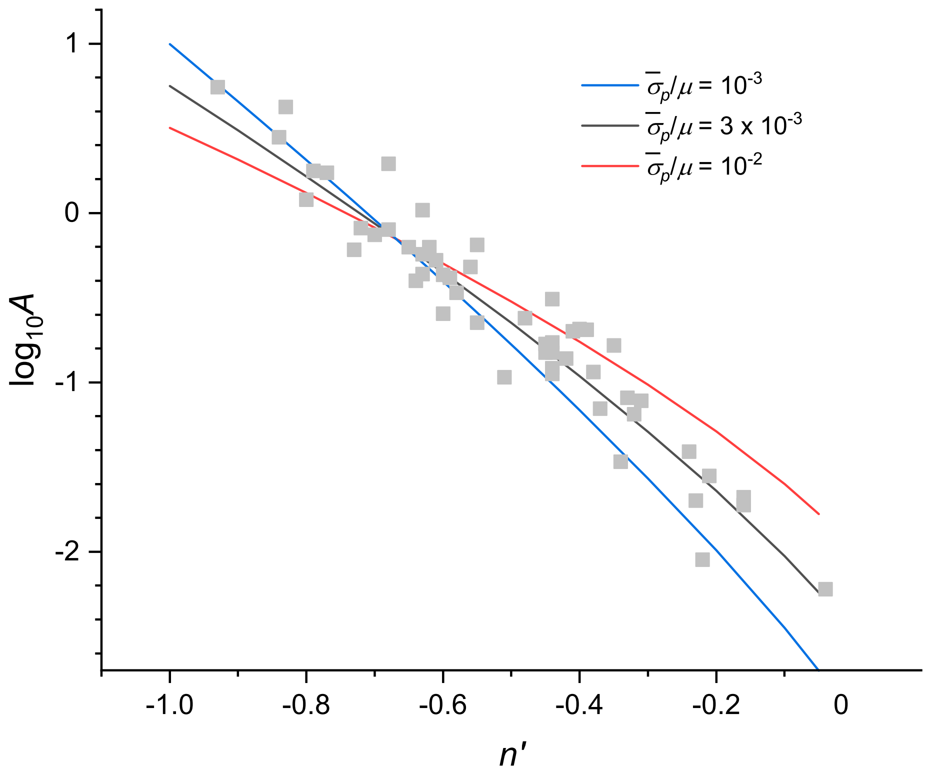

Figure 2. Influence of the mean flow stress value, $\overline{\sigma_p}/\mu$, on equation 5 when compared with the data for bcc metal micropillar compression using $n' = -0.67$ and $A' = 0.71$.

inspection of equation 7 shows that the form of the relation is strongly influenced by the parameter n', which from equation 3 and equation 6 is the proposed 'intrinsic' power law of the size effect. To explore this, we have superimposed upon the experimental data presented in Figure 1b three lines that represent: n' = –1, expected if the power law is related directly to the diameter of the pillar (e.g. the single arm source mechanism; [18] n' = −0.67), the mean value reported with data from fcc pillars; [13,14] and n' = –0.5, if the mechanism follows a mechanism similar to barrier penetration, e.g. a critical dislocation pile up and release. As can be seen, the line representing n' = –0.67 shows the closest agreement with the data. This suggests that both fcc and bcc metals obey the same mechanism for the size effect, but this observation does not provide sufficient information to identify it.

Note that to generate the lines shown on Figure 1b from equation 5, the following additional assumptions are made: (1) A' = 0.71, this has been selected because it is the average pre-exponent determined from fcc data reviewed by Dou and Derby [14]. (2) $\overline{\sigma_p} = 3 \times 10^{-3}$, this has been selected because most micropillar compression experiments of bcc and fcc metals reported in the literature have been carried out in the approximate range of $10^{-3} < \sigma_p/\mu < 10^{-2}$

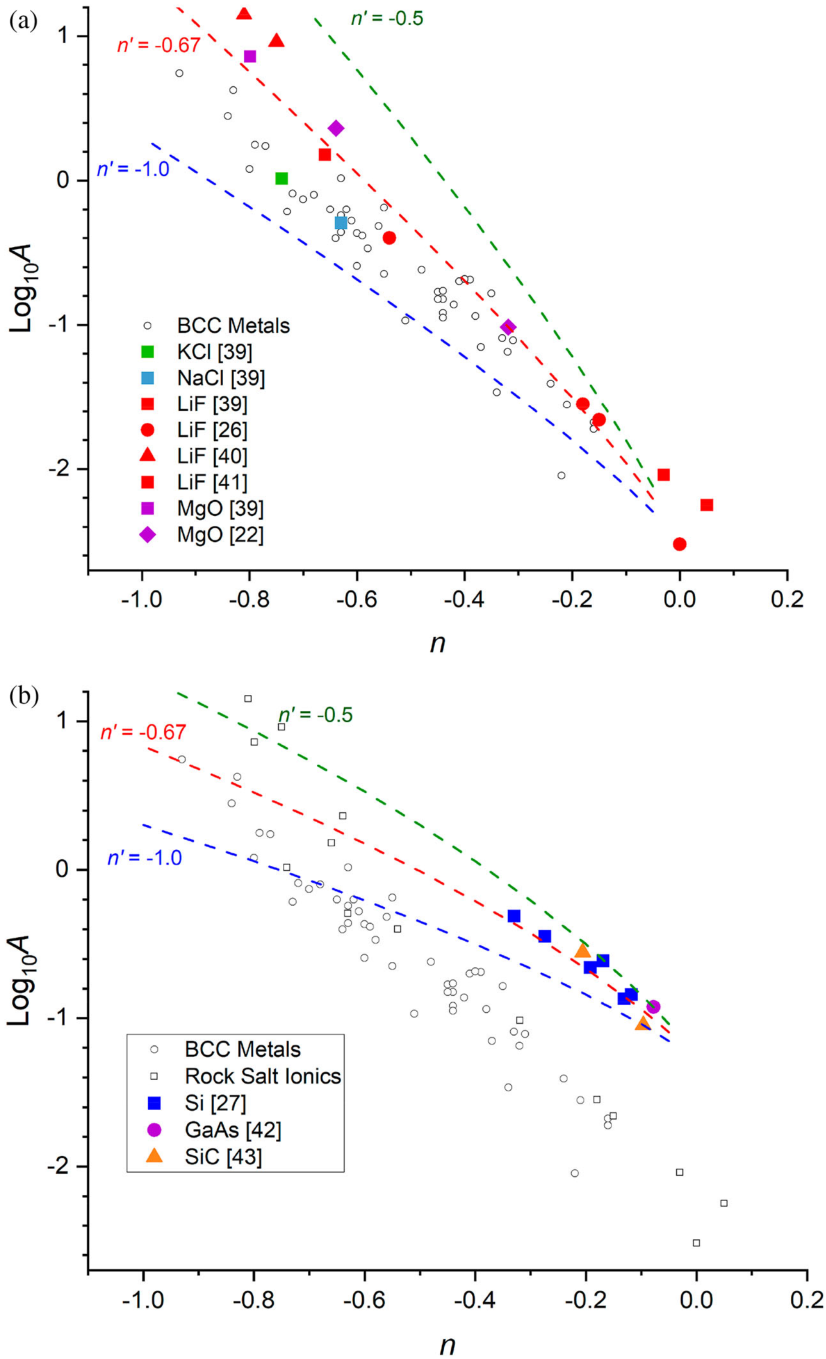

Figure 3. The correlation between the power law exponent, *n*, and the pre-exponential constant, *A* for materials with: a) The rock salt (NaCl) crystal structure; the bcc data from Figure 1a is included for comparison. b) Semiconductors with structures based on diamond or related hexagonal structures (SiC is the 6H structure) with bcc and rock salt structures shown for reference. The dotted lines are plots of equation 7 for different values of the intrinsic size exponent, *n′*, with constants from Table 1.

Table 1. Constants used in equation 7 to describe the correlation between the size effect exponent, n, and the pre-exponential constant, A.

Material class	$\overline{\sigma_p}/\mu$	A′
BCC Metals	3×10^{-3}	0.71
NaCl Structure Ionic Crystals	3×10^{-3}	1.00
Covalent Semiconductors	5×10^{-2}	2.00

(see Supplementary Information Figures S1 and S2). The effect of using either of these limiting values of $\overline{\sigma_p}/\mu$ on the agreement with data is shown in Figure 2 and the effect of this on the correlation with n' = -0.67 is small.

2.2 Ionic solids and semiconductors

Another set of crystalline materials that display temperature activation of slip are ionic crystals that form the Rock Salt structure. These show different deformation behaviour, dependent on the active slip system. These are termed soft slip that occurs when the active slip system is of type {110}$1\bar{1}0$ and hard slip when the system is {100}$1\bar{1}0$. The behaviour of a number of these materials tested in micropillar compression has been reviewed by Zou and Spolenak [39] They found that tests on pillars, oriented to favour soft slip, displayed a size effect similar to that found with fcc metals and those oriented for hard slip showed a reduced size effect with exponents similar to those found with bcc materials. A similar conclusion on the behaviour of MgO crystals in micropillar compression oriented for either hard or soft slip was also found by Korte and Clegg [22] A more detailed study of the behaviour of LiF micropillars tested over a range of temperatures by Soler et al. [26] also demonstrated that the size sensitivity of pillars oriented for hard slip tended to that of the fcc metals as the testing temperature increased and allowed thermal activation of the hard slip systems. This is clearly similar to the thermal activation of slip in bcc metals. There is a more limited set of micropillar compression experiments in the literature on semiconductor materials with the diamond cubic and related crystal structures. Of these, there have been studies of the effect of pillar diameter on flow stress for Si, GaAs and SiC [27,40,41] The micropillar size/strength exponent, n, and pre-exponent, A, reported for micropillar compression experiments carried out on materials with the rock salt crystal structure and a range of semiconductors have been determined using the published data or by digitising appropriate plots and normalising with the Burgers vector and appropriate single crystal elastic constants. These are tabulated in Table S2 and displayed in Figure 3, superimposed upon the general data for bcc materials for comparison purposes. There are fewer data points than available for bcc metals but as in both cases there appears to be a strong correlation between n and the pre-exponent, A.

For both classes of materials presented in Figure 3, the correlation between n and A can be described by equation 7 but with slightly different values for the constants A' and $\overline{\sigma_p}/\mu$ than provided the best fit for the data obtained from the bcc metals. The values used for these constants in all three cases are presented in Table 1. For all cases we consider the intrinsic size effect, n', to be in the range $-1.0 < n' -0.5$ because this encompasses the likely values for known size effects in strengthening mechanisms. The mean stress, $\overline{\sigma_p}/\mu$, is determined by the range of stresses over which the experimental data is measured. The literature data for ionic crystals covers a similar range of normalised stress as reported for fcc and bcc metals, see Supplementary Information Figure S3. However, the covalent nature of bonding in semiconductor crystals leads to a much greater lattice resistance for slip, hence the range of normalised stress needed for micropillar compression testing is correspondingly greater, see Supplementary Information Figure S4. Thus, for the ionic crystal data we have used thus $\overline{\sigma_p}/\mu = 3 \times 10^{-3}$ (the same as for bcc metals) and for semiconductors $\overline{\sigma_p}/\mu = 5 \times 10^{-2}$. Using these values the best fit to experimental data was obtained using $A' = 1.0$ and $A' = 2.0$ for ionic crystals and semiconductors respectively. This compilation of the current experimental data in the literature is consistent with all three materials classes considered showing identical power law behaviour.

We note that in this compilation of literature there can be considerable inconsistency between the measurements we have recorded from the literature from different studies of the same material. There is no standard procedure adopted between the different groups who have used micropillar compression to determine the mechanical properties of small diameter pillars. Potential inconsistencies and sources of statistical scatter include:

1) The strain at which the plastic flow stress is measured – it can be difficult to identify a distinct yield point from the experimental stress strain curves measured in the reported studies. As can be seen from the Supplementary Material Tables S1, S2 and S3, the flow stress is described as either the onset of plasticity or after a fixed strain ranging from 0.2 to 8%.
2) The orientation of the pillar compression axis. The pillars are normally reported as along a crystallographically significant low index axis, e.g. [001], [011] or [111]. However, the pillars are fabricated using ion beam milling and often from polycrystalline specimens where grain orientation is determined experimentally, thus there is normally a small uncertainty in the actual loading direction and hence in accurately determining the stress resolved on an appropriate slip system.
3) In addition, the milling process may result in a small taper in the pillar diameter, with the stress normally computed using the diameter of the top of the pillar.

However, we do not believe that these uncertainties significantly alter the trends and correlations we have identified. Indeed, a similar conclusion concerning data accuracy is reached by Dunstan and Bushby [28] in their analysis of data to justify their interpretation of size dependent mechanical properties in the broadest sense.

Finally, we return to the argument of Dunstan and Bushby, [28] who strongly argue that there is an intrinsic limit to the elastic strain limit (the strain at which plastic deformation initiates) and a dimensional scale normalised by the atomic spacing of the crystal (effectively identical to the Burgers vector for the case of metals). As discussed earlier this argument is restating equation 2 but with an exponent of -1 and a pre-exponent of 1. They argue that as all experimental data from a range of experiments lies to the right of this locus (presented in their publication Figure 6 [28]), it represents an intrinsic size limit to deformation (a minimum deformation stress) and all size effects reported in the literature, whether imposed by strain gradients or by geometric confinement of dislocations, are in addition to their limiting locus in the strain/size parameter space. We note that their argument does not eliminate the possibility of a size dependent strengthening mechanism for micropillar compression with a scale dependence exponent > -1.0, it defines a minimum strength size scale limit, and they accept that there are strengthening mechanisms that must explain the data showing strengths greater than their limiting locus. If Dunstan and Bushby's limiting strength were solely the case, we would expect our data for the correlation between the empirical constants, n and A, to show a gradient more strongly correlated with $n' = -1.0$, rather than a value $-1.0 < n' < -0.5$, found with our selection of data from metals and inorganic solids.

3. Conclusions

An analysis of the literature for the micro-compression testing of bcc metal pillars, ionic crystals with the rock salt (NaCl) structure, and covalently bonded semiconductors, finds that they have many similarities in their size dependent behaviour. In all cases the size dependence can be described by a simple empirical power law relating the plastic flow stress to the pillar diameter. We have demonstrated that, when the flow stress is normalised by the shear modulus resolved on the slip plane, σ_p/μ, and the pillar diameter is normalised by the Burgers' vector of the active slip system, d/b, such that the power law is described by equation 2:

$$\frac{\sigma_p}{\mu} = A\left(\frac{d}{b}\right)^n \tag{8}$$

There is a strong correlation between the exponent, n, and the logarithm of the pre-exponential constant, A. This correlation can itself be described by a further empirical equation (equation 7) with

$$logA = \log\frac{\overline{\sigma_p}}{\mu} - \frac{n}{n'}\left[\log\frac{\overline{\sigma_p}}{\mu} + log\frac{n}{n'} - logA'\right] \quad (9)$$

Here the constant n' represents a universal power law that is common to all materials and in each of the three classes of materials investigated, it lies in the range $-1.0 < n' < -0.5$. These bounding values are the same as would be predicted if the strengthening is controlled by a dislocation bowing mechanism ($n' = -1.0$), e.g. a single arm dislocation source [12], or if the strengthening is controlled by the penetration of a barrier or a critical energy release mechanism ($n' = -0.5$). This correlation is consistent with an equation of the following form providing a description of the size dependent behaviour of the strength measures in micropillar compression experiments (equation 10)

$$\frac{\sigma_p - \sigma_b}{\mu} = A'\left(\frac{d}{b}\right)^{n'} \quad (10)$$

Where σ_b is a size independent or 'bulk' stress that impedes plastic flow and contains contributions from microstructural features, such as pre-existing dislocation density and any intrinsic lattice resistance to dislocation motion. Our results are consistent with the exponent, n', being common to at least three materials types (bcc metals, ionic compounds with the NaCl structure and covalent semiconductors) but with the constant A' showing some small variation. We note also that the data is also consistent with the limiting elastic strain model of Dunstan and Bushby [28] but this would also imply the limiting value of $n' = -1$. Although these results do not identify the mechanism for the size effect observed during micropillar compression experiments, the uniform behaviour described here across three different classes of materials provides strong evidence for a common mechanism operating.

Disclosure statement

No potential conflict of interest was reported by the author(s).

Funding

This work was supported by Engineering and Physical Sciences Research Council: [Grant Numbers EP/J021229/1, EP/S009493/1, EP/R00661X/1, EP/S019367/1, EP/P025021/1, and EP/P025498/1].

ORCID

Brian Derby http://orcid.org/0000-0001-5753-0166

References

[1] J.W. Matthews and J.L. Crawford, *Accommodation of misfit between single-crystal films of nickel and copper*. Thin Solid Films 5 (1970), pp. 187–198. doi:10.1016/0040-6090(70)90076-3.

[2] D.J. Dunstan, S. Young, and R.H. Dixon, *Geometrical theory of critical thickness and relaxation in strained-layer growth*. J. Appl. Phys 70 (1991), pp. 3038–3045. doi:10.1063/1.349335.

[3] N.A. Fleck, G.M. Muller, M.F. Ashby, and J.W. Hutchinson, *Strain gradient plasticity: theory and experiment*. Acta Metall. Mater. 42 (1994), pp. 475–487. doi:10.1016/0956-7151(94)90502-9.

[4] J.S. Stölken and A.G. Evans, *A microbend test method for measuring the plasticity length scale*. Acta Mater. 46 (1998), pp. 5109–5115. doi:10.1016/S1359-6454(98)00153-0.

[5] W.D. Nix and H. Gao, *Indentation size effects in crystalline materials: A law for strain gradient plasticity*. J. Mech. Phys. Solids 46 (1998), pp. 411–425. doi:10.1016/S0022-5096(97)00086-0.

[6] M.F. Ashby, *The deformation of plastically non-homogeneous materials*. Philosophical Mag. A 21 (1970), pp. 399–424.

[7] D.M.D. Uchic, J.N. Florando, and W.D. Nix, *Sample dimensions influence strength and crystal plasticity*. Science 305 (2004), pp. 986–989. doi:10.1126/science.1098993.

[8] J.R. Greer, W.C. Oliver, and W.D. Nix, *Size dependence of mechanical properties of gold at the micron scale in the absence of strain gradients*. Acta Mater. 53 (2005), pp. 1821–1830. doi:10.1016/j.actamat.2004.12.031.

[9] C.A. Volkert and E.T. Lilleodden, *Size effects in the deformation of sub-micron Au columns*. Philos. Mag 86 (2006), pp. 5567–5579. doi:10.1080/14786430600567739.

[10] D. Kiener, C. Motz, T. Schoeberl, M. Jenko, and G. Dehm, *Determination of mechanical properties of copper at the micron scale*. Adv. Engin. Mater 8 (2006), pp. 1119–1125. doi:10.1002/adem.200600129.

[11] R. Dou and B. Derby, *The strength of Au nanowire forests*. Scripta Mater 59 (2008), pp. 151–154. doi:10.1016/j.scriptamat.2008.02.046.

[12] R. Dou and B. Derby, *A universal scaling law for the strength of metal micropillars and nanowires*. Scripta Mater 61 (2009), pp. 524–527. doi:10.1016/j.scriptamat.2009.05.012.

[13] J. Greer and J.T.M. de Hosson, *Plasticity in small-sized metallic systems: Intrinsic versus extrinsic size effect*. Prog. Mater. Sci 56 (2011), pp. 654–724. doi:10.1016/j.pmatsci.2011.01.005.

[14] E. Arzt, *Size effects in materials due to microstructural and dimensional constraints: a comparative review*. Acta Mater. 46 (1998), pp. 5611–5626. doi:10.1016/S1359-6454(98)00231-6.

[15] J.R. Greer and W.D. Nix, *Nanoscale gold pillars strengthened through dislocation starvation*. Phys. Rev. B 73 (2006), pp. 245410). doi:10.1103/PhysRevB.73.245410.

[16] Z.W. Shan, R.K. Mishra, S.A. Syed Asif, O.L. Warren, and A.M. Minor, *Mechanical annealing and source-limited deformation in submicrometre-diameter Ni crystals*. Nature Mater. 7 (2008), pp. 115–119. doi:10.1038/nmat2085.

[17] D. Kiener and A.M. Minor, *Source truncation and exhaustion: insights from quantitative in situ TEM tensile testing*. Nano. Lett 11 (2011), pp. 3815–3820. doi:10.1021/nl201890s.

[18] T.A. Parthasarathy, S.I. Rao, D.M. Dimiduk, M.D. Uchic, and D.R. Trinkle, *Contribution to size effect of yield strength from the stochastics of dislocation source*

lengths in finite samples. Scripta Mater 56 (2007), pp. 313–316. doi:10.1016/j.scriptamat.2006.09.016.

[19] S. Brinckmann, J.Y. Kim, and J.R. Greer, *Fundamental differences in mechanical behavior between two types of crystals at the nanoscale*. Phys. Rev. Lett 100 (2008), pp. 155502). doi:10.1103/PhysRevLett.100.155502.

[20] A.S. Schneider, B.G. Clark, C.P. Frick, P.A. Gruberd, and E. Arzt, *Effect of orientation and loading rate on compression behavior of small-scale Mo pillars*. Mater. Sc. Eng. A 505 (2009), pp. 241–246. doi:10.1016/j.msea.2009.01.011.

[21] A.S. Schneider, D. Kaufmann, B.G. Clark, C.P. Frick, P.A. Gruber, R. Mönig, O. Kraft, and E. Arzt, *Correlation between Critical Temperature and Strength of Small-Scale bcc Pillars*. Phys. Rev. Lett. 103 (2009), pp. 105501). doi:10.1103/PhysRevLett.103.105501.

[22] S. Korte and W.J. Clegg, *Discussion of the dependence of the effect of size on the yield stress in hard materials studied by microcompression of MgO*. Phil. Mag. 91 (2011), pp. 1150–1162. doi:10.1080/14786435.2010.505179.

[23] S.W. Lee and W.D. Nix, *Size dependence of the yield strength of fcc and bcc metallic micropillars with diameters of a few micrometers*. Phil. Mag. 92 (2012), pp. 1238–1260. doi:10.1080/14786435.2011.643250.

[24] O.T. Abad, J.M. Wheeler, J. Michler, A.S. Schneider, and E. Arzt, *Temperature-dependent size effects on the strength of Ta and W micropillars*. Acta Mater. 103 (2016), pp. 483–494. doi:10.1016/j.actamat.2015.10.016.

[25] H. Yilmaz, C.J. Williams, J. Risan, and B. Derby, *The size dependent strength of Fe, Nb and V micropillars at room and low temperature*. Materialia **7** (2019), pp. 100424). doi:10.1016/j.mtla.2019.100424.

[26] R. Soler, J.M. Wheeler, H.J. Chang, J. Segurado, J. Michler, J. LLorca, and J.M. Molina-Aldareguia, *Understanding size effects on the strength of single crystals through high-temperature micropillar compression*. Acta Mater. 81 (2014), pp. 50–57. doi:10.1016/j.actamat.2014.08.007.

[27] M. Chen, J. Wehrs, A.S. Sologubenko, J. Rabier, J. Michler, and J.M. Wheeler, *Size-dependent plasticity and activation parameters of lithographically-produced silicon micropillars*. Mater. Design 189 (2020), pp. 108506). doi:10.1016/j.matdes.2020.108506.

[28] D.J. Dunstan and A.J. Bushby, *The scaling exponent in the size effect of small scale plastic deformation*. Inter. J. Plasticity 40 (2013), pp. 152–162. doi:10.1016/j.ijplas.2012.08.002.

[29] B.R.S. Rogne and C. Thaulow, *Effect of crystal orientation on the strengthening of iron micro pillars*. Mater. Sci. Eng. A 621 (2015), pp. 133–142. doi:10.1016/j.msea.2014.10.067.

[30] R. Huang, Q.-J. Li, Z.-J. Wang, L. Huang, J. Li, E. Ma, and Z.-W. Shan, *Flow stress in submicron BCC iron single crystals: sample-size-dependent strain-rate sensitivity and rate-dependent size strengthening*. Mater. Res. Lett 3 (2015), pp. 121–127. doi:10.1080/21663831.2014.999953.

[31] H. Yilmaz, C.J. Williams, and B. Derby, *Size effects on strength and plasticity of ferrite and austenite pillars in a duplex stainless steel*. Mater. Sci. Eng. A 793 (2020), pp. 139883). doi:10.1016/j.msea.2020.139883.

[32] H. Yilmaz. Mechanical properties of body-centred cubic nanopillars. Ph.D. Thesis, University of Manchester, Manchester, UK (2018).

[33] A.S. Schneider, C. Frick, E. Arzt, W. Clegg, and S. Korte, *Influence of test temperature on the size effect in molybdenum small-scale compression pillars*. Phil. Mag. Lett 93 (2013), pp. 331–338. doi:10.1080/09500839.2013.777815.

[34] J.-Y. Kim, D. Jang, and J.R. Greer, *Tensile and compressive behavior of tungsten, molybdenum, tantalum and niobium at the nanoscale*. Acta Mater. 58 (2010), pp. 2355–2363. doi:10.1016/j.actamat.2009.12.022.

[35] S.M. Han, T. Bozorg-Grayeli, J.R. Groves, and W.D. Nix, *Size effects on strength and plasticity of vanadium nanopillars*. Scr. Mater. 63 (2010), pp. 1153–1156. doi:10.1016/j.scriptamat.2010.08.011.

[36] A.S. Schneider, C. Frick, B. Clark, P. Gruber, and E. Arzt, *Influence of orientation on the size effect in bcc pillars with different critical temperatures*. Mater. Sci. Eng. A 528 (2011), pp. 1540–1547. doi:10.1016/j.msea.2010.10.073.

[37] S.-W. Lee, Y. Cheng, I. Ryu, and J. Greer, *Cold-temperature deformation of nano-sized tungsten and niobium as revealed by in-situ nano-mechanical experiments*. China Technol. Sci 57 (2014), pp. 652–662. doi:10.1007/s11431-014-5502-8.

[38] D. Kaufmann, R. Mönig, C. Volkert, and O. Kraft, *Size dependent mechanical behaviour of tantalum*. J. Plasticity 27 (2011), pp. 470–478. doi:10.1016/j.ijplas.2010.08.008.

[39] Y. Zou and R. Spolenak, *Size-dependent plasticity in micron- and submicron-sized ionic crystals*. Phil. Mag. Lett 93 (2013), pp. 431–438. doi:10.1080/09500839.2013.797616.

[40] E.M. Nadgorny, D.M. Dimiduk, and M.D. Uchic, *Size effects in LiF micron-scale single crystals of low dislocation density*. J. Mater. Res 23 (2008), pp. 2829–2835. doi:10.1557/JMR.2008.0349.

[41] R. Soler, J.M. Molina-Aldareguia, J. Segurado, J. Llorca, R.I. Merino, and V.M. Orera, *Micropillar compression of LiF [111] single crystals: Effect of size, ion irradiation and misorientation*. Inter. J. Plasticity 36 (2012), pp. 50–63. doi:10.1016/j.ijplas.2012.03.005.

[42] F. Östlund, P.R. Howie, R. Ghisleni, S. Korte, K. Leifer, W.J. Clegg, and J. Michler, *Ductile-brittle transition in micropillar compression of GaAs at room temperature*. Philos. Mag 91 (2011), pp. 1190–1199. doi:10.1080/14786435.2010.509286.

[43] K. Kishida, Y. Shinkai, and H. Inui, *Room temperature deformation of 6H–SiC single crystals investigated by micropillar compression*. Acta Mater. 187 (2020), pp. 19–28. doi:10.1016/j.actamat.2020.01.027.

[44] R. Fritz, V. Maier-Kiener, D. Lutz, and D. Kiener, *Interplay between sample size and grain size: Single crystalline vs. ultrafine-grained chromium micropillars*. Mater. Sci. Eng. A 674 (2016), pp. 626–633. doi:10.1016/j.msea.2016.08.015.

[45] D. Kiener, R. Fritz, M. Alfreider, A. Leitner, R. Pippan, and V. Maier-Kiener, *Rate limiting deformation mechanisms of bcc metals in confined volumes*. Acta Mater. 166 (2019), pp. 687–701. doi:10.1016/j.actamat.2019.01.020.